Probabilistic invasion maps of pyroclastic density current hazard by using long-term vent opening mapping and simplified invasion models: application to Campi Flegrei caldera (Italy)

A. Bevilacqua[1,2], A. Neri[2] , A. Bertagnini[2], M. Bisson[2], T. Esposti Ongaro[2], C. Fourmentraux[2], F. Flandoli[3], E. Iannuzzi[4], R. Isaia[5], S. Orsucci [6], M. Rosi[4], C. Scirocco[7], S. Vitale[7]

(1) Scuola Normale Superiore, Pisa
(2) Istituto Nazionale di Geofisica e Vulcanologia, Sezione di Pisa, Pisa
(3) Università di Pisa, Dip.to di Matematica Applicata, Pisa
(4) Università di Pisa, Dip.to di Scienze della Terra, Pisa
(5) Istituto Nazionale di Geofisica e Vulcanologia, Osservatorio Vesuviano, Napoli
(6) Università di Pisa, Dip.to di Fisica, Pisa
(7) Università di Napoli Federico II, Dip.to di Scienze della Terra, dell'Ambiente e delle Risorse, Napoli

FIST 2013
IX Forum Italiano di Scienze della Terra
Pisa, 16-18 September 2013

INGV SCUOLA NORMALE SUPERIORE PISA UNIVERSITÀ DI PISA

The objective

The PDC hazard mapping in the CF caldera is particularly challenging due to

- 1) the large uncertainty on **future vent location**
- 2) the unpredictable **scale of future activity**, and
- 3) the **complex dynamics of PDC** (particularly over the 3D caldera topography)

Satellite image of Campi Flegrei caldera (Bisson et al., 2007)

A **quantitative probabilistic mapping of PDC invasion**, possibly able to account for the **intrinsic uncertainties** of the system, is needed for hazard assessment.

We focused our work on the **quantification of the different sources of uncertainty** in order to produce median and quantile probabilistic maps.

The methodology

In order to produce a long-term probability map of PDC hazard of the CF caldera we **considered the main sources of uncertainty** by using ***probability density functions*** and ***simplified PDC invasion models***.
In particular, we used:

•a **probability map of new vent opening** using new field work and mathematical modelling about past eruptive activity and caldera volcanological features.

•a **probability law describing the distribution of eruptive scales (i.e. PDC invasion areas)** of past events at CF
(i.e. we do not need to select a specific reference scenario)

• **simplified PDC invasion models**

The final invasion map was obtained by ***Monte Carlo simulation*** by sampling the possible events w.r.t. the above pdf distributions.
Whenever possible probability distributions were considered together with the ***associated uncertainties***.

The production of the probabilistic vent opening map

We based on the assumption that the probability of vent opening can be expressed as a **weighted combination of spatial distributions of relevant variables** (i.e. past vents, faults and fractures).

In particular we focused on the quantification of some sources of uncertainty such as:

- Uncertainty on the spatial location of eruptive vents/fissures (with reference to the last 15 kyrs)

- Uncertainty due to the incompleteness of the datasets of the variables considered (i.e. past vent openings, faults and fractures)

- Uncertainty on the relative weights of the different variables considered

Vent opening data with uncertainty

Epoch I: 33 vents (about 10.6-15 kyrs ago)

1	Bellavista
2	Mofete
3	Gauro
4	Santa_Teresa
5	La_Pietra
6	La_Pigna1
7	La_Pigna2
8	Torre_cappella
9	Minopoli1
10	Paradiso
11	Soccavo1
12	Gaiola
13	Pomici_Principal
14	Paleo_Pisani1
15	Paleo_Pisani2
16	Soccavo2
17	Soccavo3
18	S4s3_1
19	S4s3_2
20	Soccavo4
21	Paleo_SanMartino
22	Minopoli2
23	Soccavo5
24	Pisani1
25	Pisani2
26	Fondo_Riccio
27	Concola
28	Montagna_Spaccat
29	Pignatiello1
30	Pisani3
31	Casale
32	Bacoli
33	Porto_Miseno

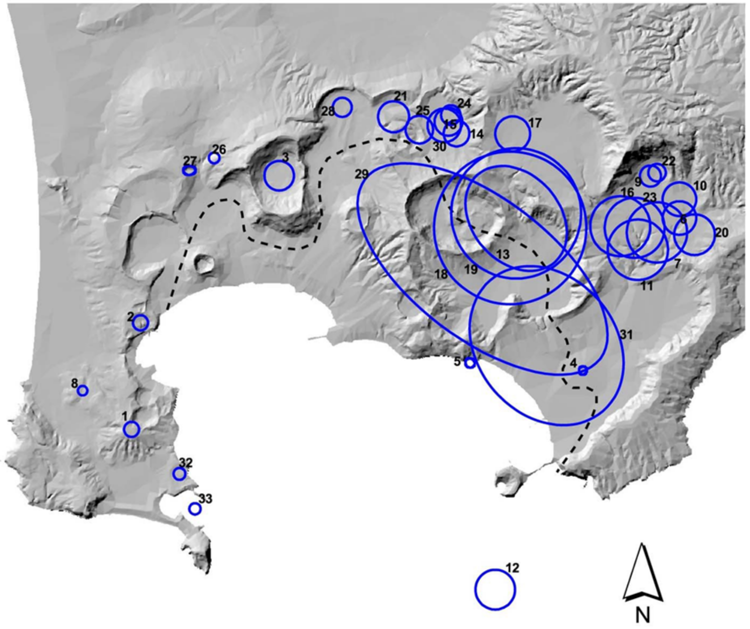

Epoch III and Mt Nuovo: 29 vents
(about 3.5-5.5 kyrs ago and 1538 AD)

1	Agnano1
2	Averno1
3	Agnano2
4	Agnano3
5	Cigliano
6	Pignatello2
7	Capo_Miseno
8	Monte_santAngelo
9	Paleoastroni1
10	Paleoastroni2
11	Agnano_Mt_Spina
12	S_Maria_dl_Grazie
13	Mt_Olibano_lavas
14	Accademia_lavas
15	Paleoastroni3
16	Olibano
17	Paleosolfatara
18	Solfatara
19	Averno2
20	Astroni1
21	Astroni2
22	Astroni3
23	Astroni4
24	Astroni5
25	Astroni6
26	Astroni7
27	Fossa_Lupara
28	Nisida
29	Monte_Nuovo

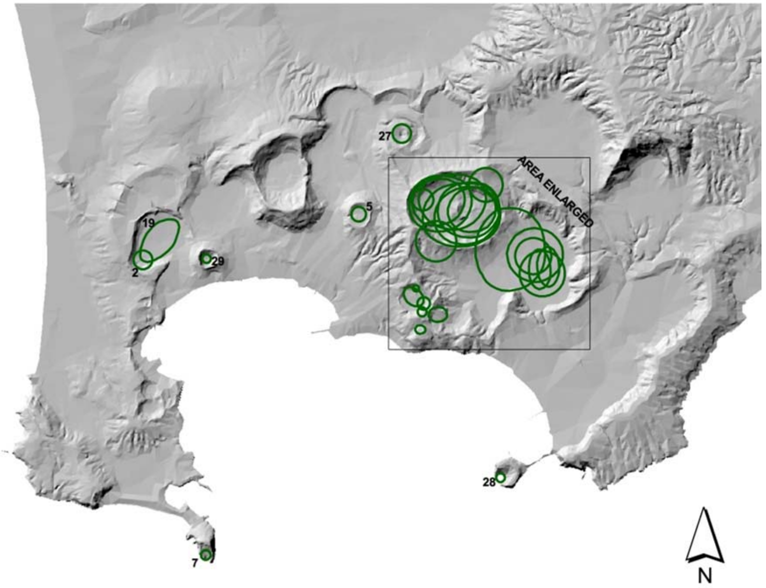

Epoch II: 8 vents (about 9.1-9.6 kyrs ago)

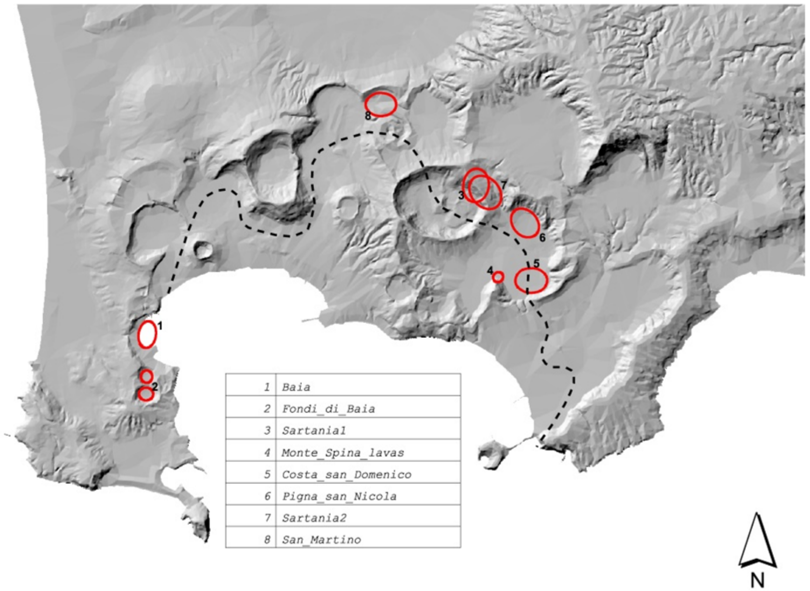

1	Baia
2	Fondi_di_Baia
3	Sartania1
4	Monte_Spina_lavas
5	Costa_san_Domenico
6	Pigna_san_Nicola
7	Sartania2
8	San_Martino

1	Agnano1
2	Averno1
3	Agnano2
4	Agnano3
5	Cigliano
6	Pignatello2
7	Capo_Miseno
8	Monte_santAngelo
9	Paleoastroni1
10	Paleoastroni2
11	Agnano_Mt_Spina
12	S_Maria_dl_Grazie
13	Mt_Olibano_lavas
14	Accademia_lavas
15	Paleoastroni3
16	Olibano
17	Paleosolfatara
18	Solfatara
19	Averno2
20	Astroni1
21	Astroni2
22	Astroni3
23	Astroni4
24	Astroni5
25	Astroni6
26	Astroni7
27	Fossa_Lupara
28	Nisida
29	Monte_Nuovo

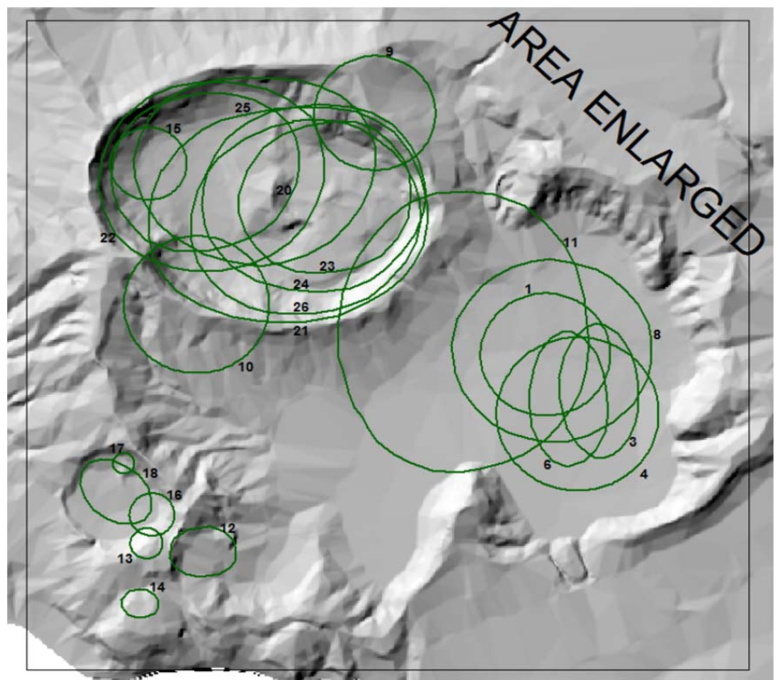

Partition of the CF caldera for vent opening

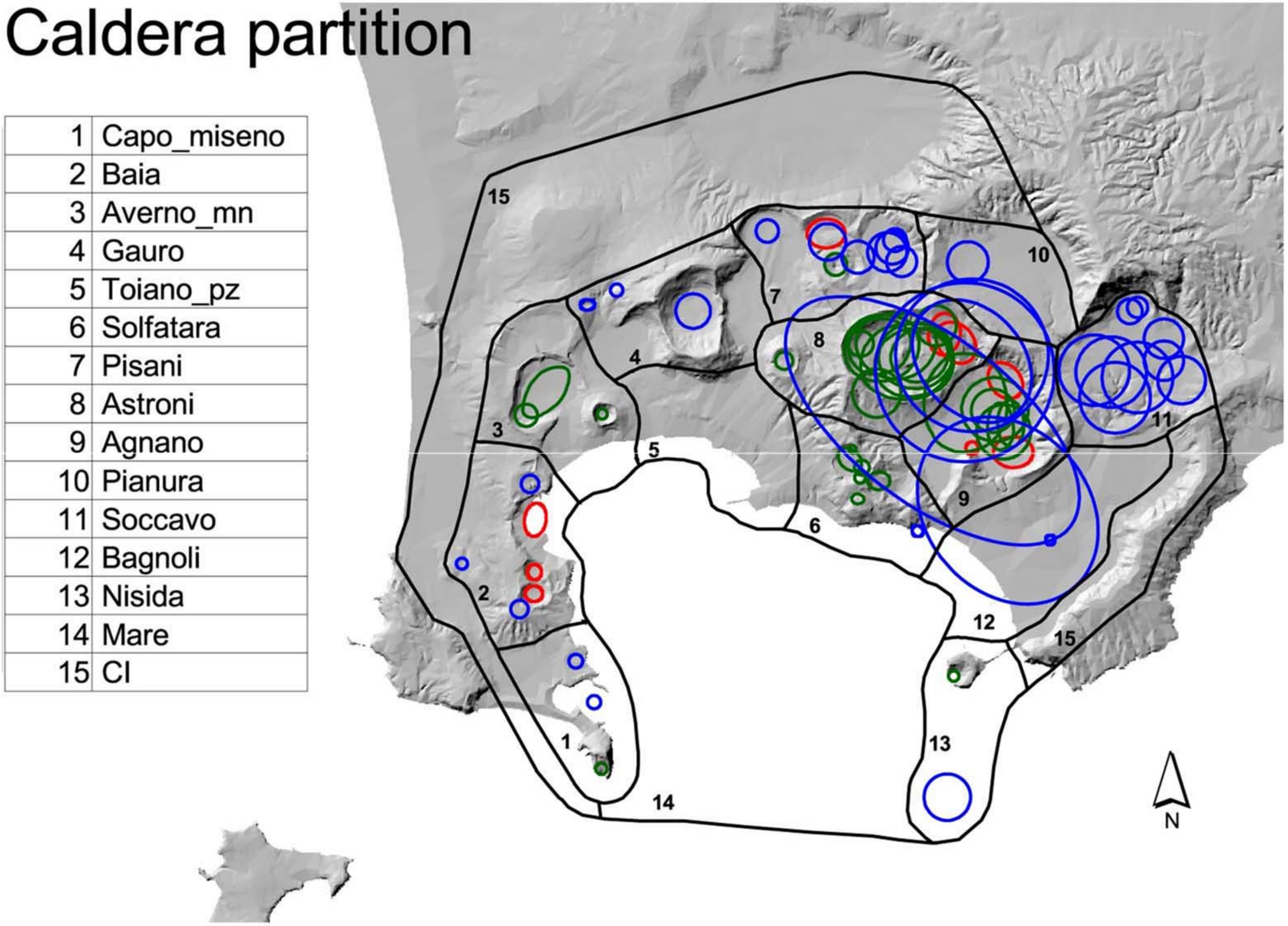

We partitioned the caldera in 15 zones by taking into account the **spatial and temporal clustering** of past vents and the actual **morphological features** of the caldera.

This has the motivation to discriminate between the zones that have a different history of activity, also based on the experts opinion.

We counted the number of ellipses contained in each zone (or the associated fraction contained) obtaining three **maps of the frequency of past vents**, one for each epoch of activity.

Distribution of faults and fractures densities

The fracture map shows the value of density of fracturation, as number of fractures per meter, obtained from discrete sampling.

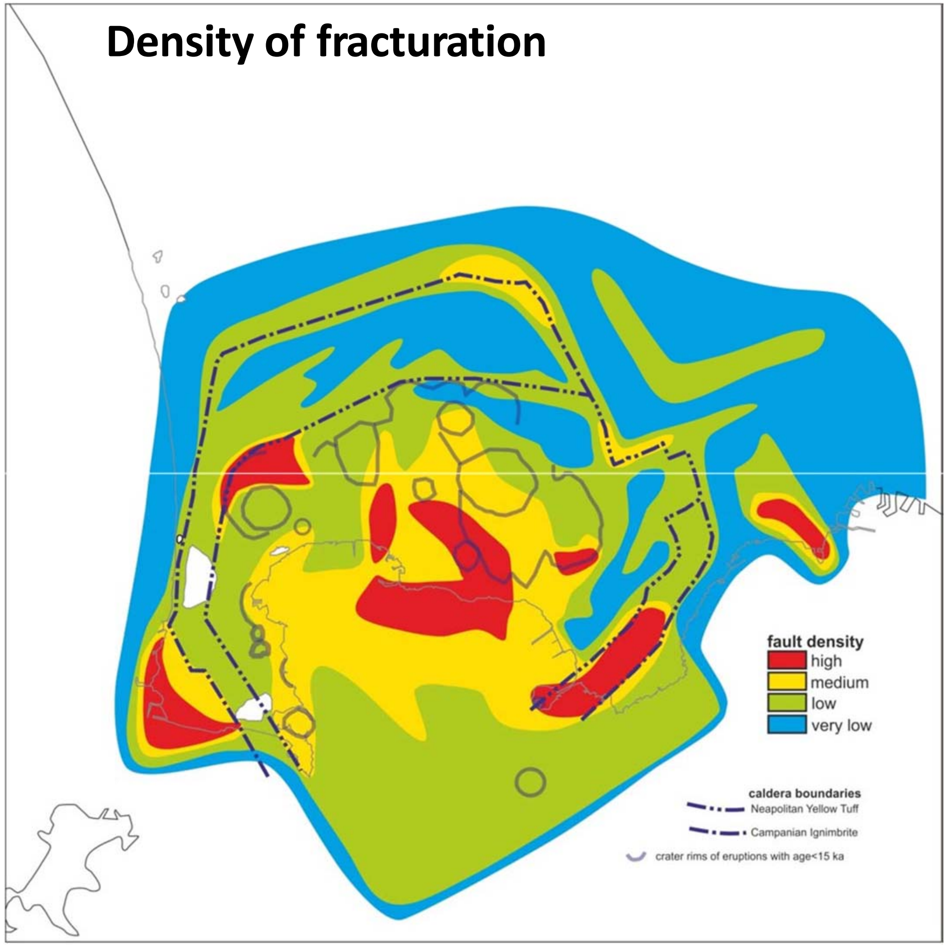

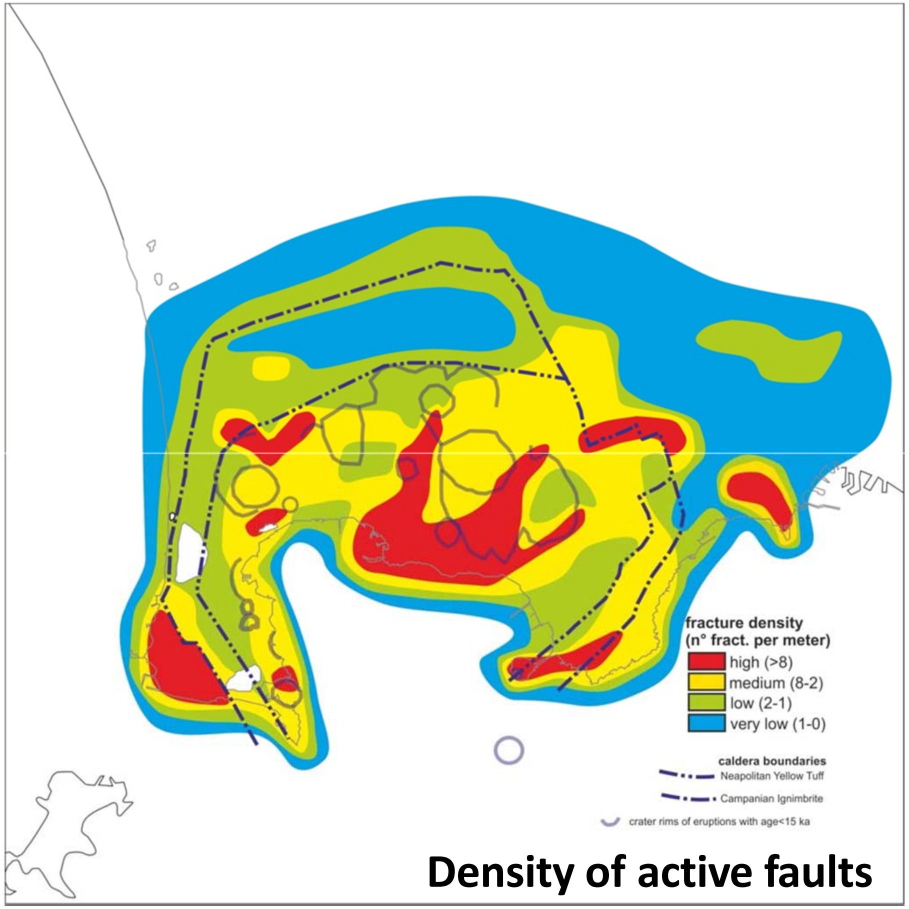

The fault map shows the value of density of faulting also including the historical deformation patterns.

Assignment of weights by expert judgement

The experts also estimated the **percentage of completeness of the datasets**. The complementary percentage (i.e. unmapped past vents, fractures and faults) was assigned to **homeogeneus maps.**

Completeness of datasets (Reliability percentage)

75%	95%	90%	80%	80%
Vents of epoch I	Vents of epoch II	Vents of epoch III	Fractures	Faults

In order to favor the assignment of weights to the geological features a **simple logic tree** was adopted (all relative weights were scaled to sum to 100%).

- **60% PAST VENTS**
  - **30% EPOCH I**
  - **30% EPOCH II**
  - **40% EPOCH III**
- **40% STRUCTURAL FEATURES**
  - **60% FRACTURES**
  - **40% FAULTS**

The weights given to the vents of the three epochs were assumed per single vent and therefore were then **normalized**.

The percentages were assigned as **modal values** and the uncertainty about them was then described using triangular distributions.

We also considered the possibility that the probability of vent opening would be correlated to other **neglected features** of the system. This has been estimated of the order of **10%.**

Preliminary probabilistic vent opening map (1)

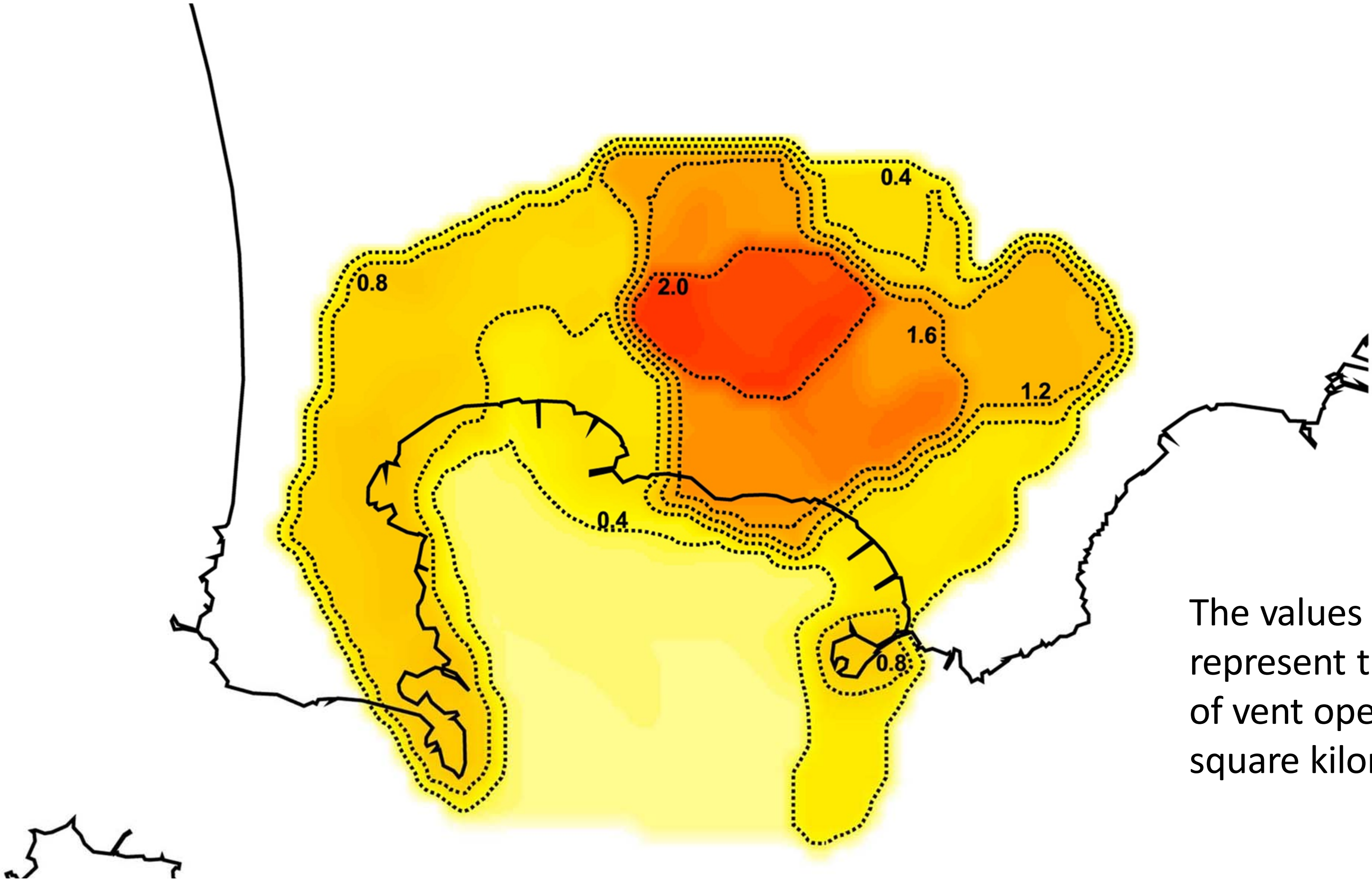

The values plotted represent the percentage of vent opening per square kilometer.

18.63%	4.83%	21.67%	17.28%	11.52%
Vents I	Vents II	Vents III	Fractures	Faults

Homogeneous maps representing lack of information — 26.07%

Preliminary probabilistic vent opening map (2)

By considering the above described uncertainty sources and using **Monte Carlo simulation** we obtained the **5% and 95%ile maps of probability of vent opening** as well as specific distributions of uncertainty in specific places.

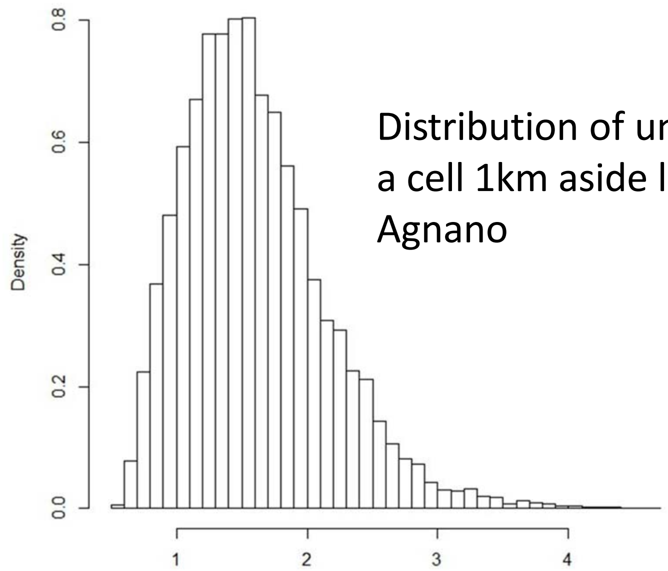

Distribution of uncertainty in a cell 1km aside located in Agnano

5th uncertainty percentile

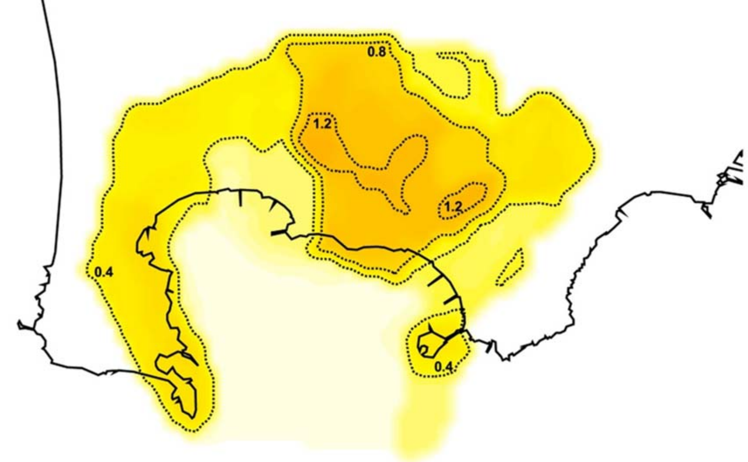

95th uncertainty percentile

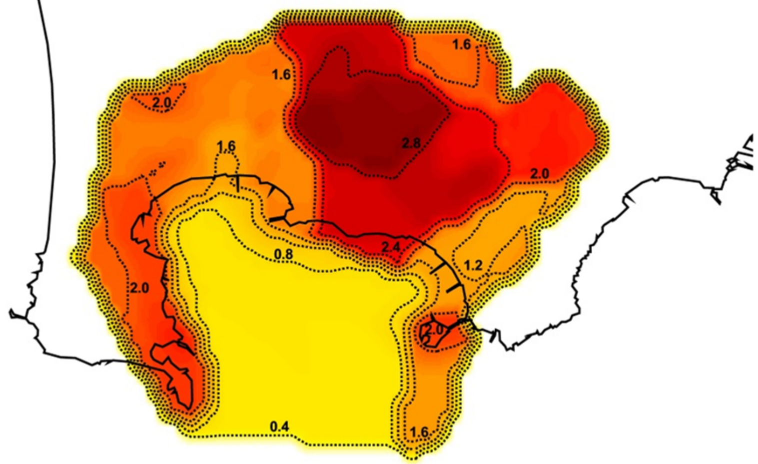

To **express the uncertainty** about the weight just given with the homogeneous maps we simulated to concentrate each part of it on single zones of the partition randomly extracted during this Monte Carlo simulation.

Probability law of the distribution of PDC invasion areas

To produce a probability law representing the scale of the eruption, we focused directly on the invaded areas of past events.

The **distribution of PDC areas** were derived from a revision of the Orsi et al. (2004) dataset.

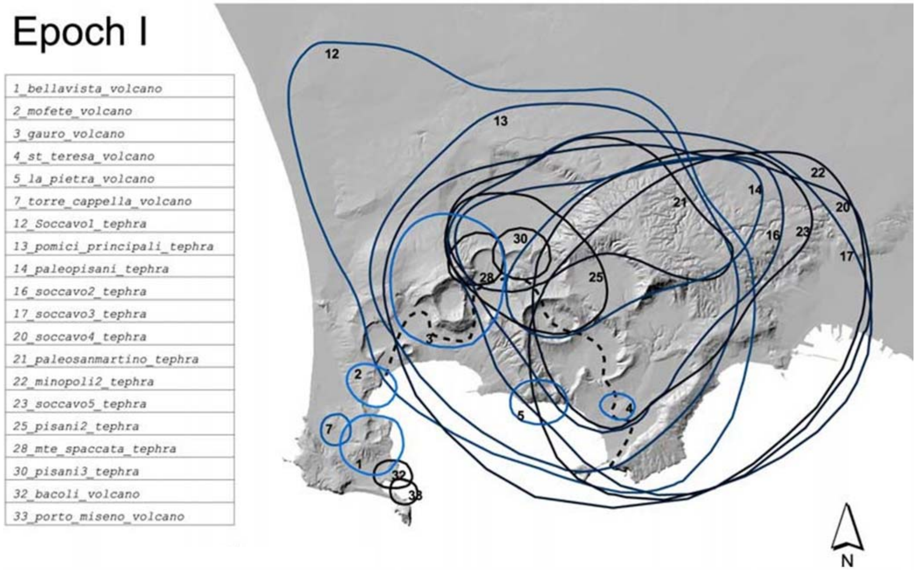

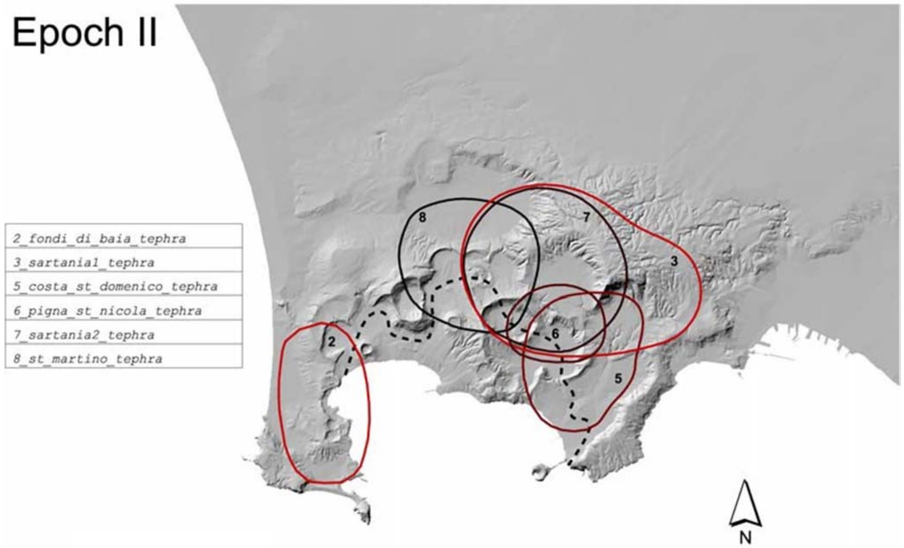

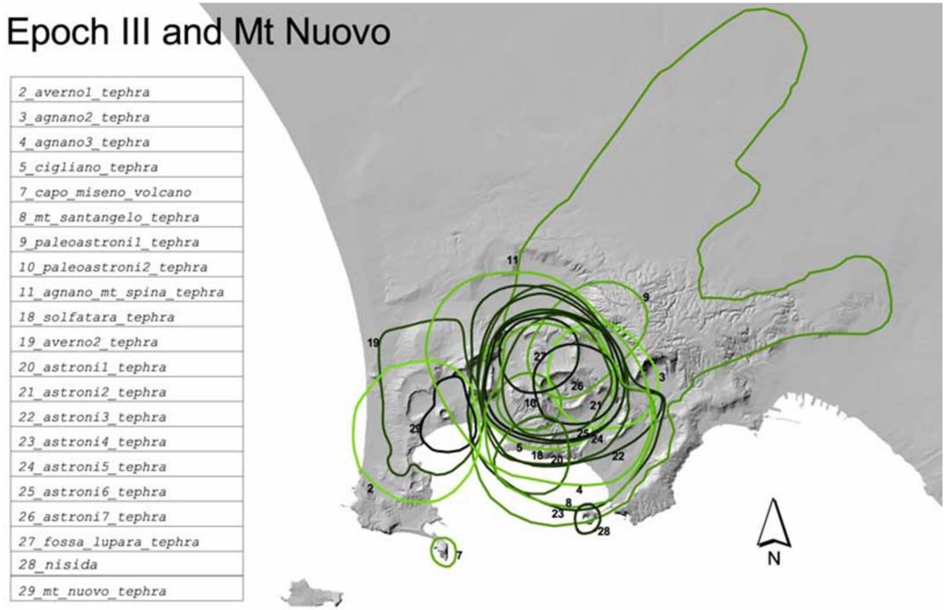

Invasion area densities were produced for **different periods** (5 vs 15 kyrs) and **probability density functions** (e.g. lognormal, etc.)

We are working to assess an uncertainty distribution also around this probability density.

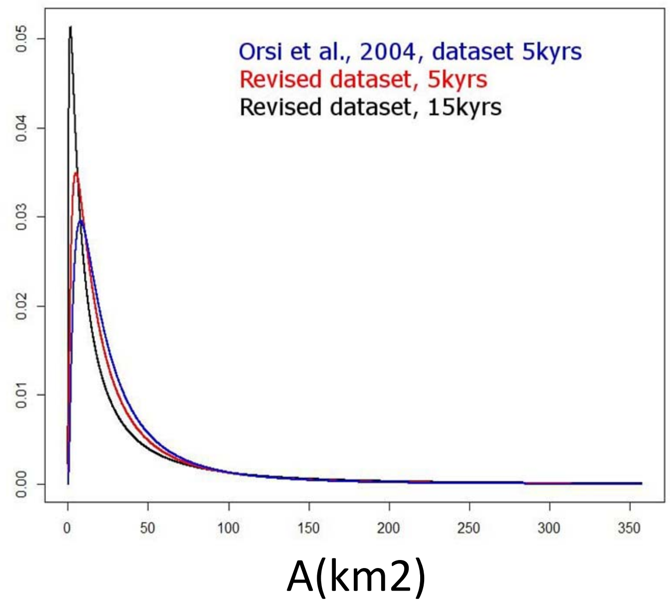

Simplified PDC invasion models

To produce probabilistic invasion maps we implemented a few ***simplified PDC invasion models*** able to describe the ***influence of caldera topography***. In particular:

•**Circular invasion area** model
(i.e. actual topographic effects neglected, accounts for an average past topography of the caldera)

•**Energy line** model (*Hsu 1975*)
(i.e. energy cone, linear decay of flow energy)

•**Box** model (*Huppert and Simpson 1980, Dade and Huppert 1996*)
calibrated by using the **2D multiphase flow model PDAC**
(*Neri et al. 2003, Esposti Ongaro et al. 2007*)

The PDC “box model”

The dynamics of the PDC are described as the **collapse of a finite volume of dense fluid in a lighter surrounding atmosphere** and on a flat surface.

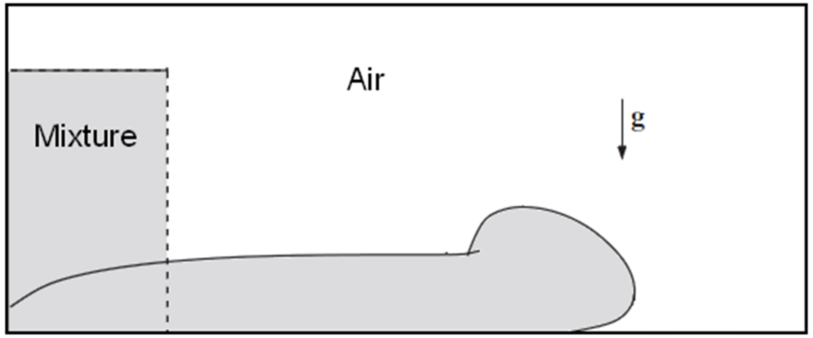

Sketch of the lock-exchange configuration

The homogeneous box model gives the **relationship between front velocity and time** as a function of initial conditions, with only one calibration parameter (Froude number, experimentally equal to 1.19) (von Karman, 1940)

For **particle-laden currents** (Huppert and Simpson, 1980):

$$\frac{\mathrm{d}L}{\mathrm{d}t} = u = \mathrm{Fr}(g'h)^{1/2}$$

$$\frac{\mathrm{d}\phi}{\mathrm{d}t} = -\frac{V_s\phi}{h}$$

$$g' = \phi g(\rho_p - \rho_a)/\rho_a \equiv \phi g_p'$$

The PDC calibrated box model (2)

Once the value of l_{max} is known, it is possible to compute the **kinetic energy of the flow front** and therefore the **height of the topographic relief that can be overcome**.

$$x = \frac{l}{l_{max}}$$

$$H^{(1)}(l, l_{max}) = \frac{1}{2g}\left[\frac{8^{-1/3} C_3 l_{max}^{1/3}}{x \cosh^2 artanh(x^2)}\right]^2$$ (axisym.)

$$C_3 = V_s^{1/3} Fr^{2/3} \phi_0^{1/3} g_p^{1/3}$$

Energy line

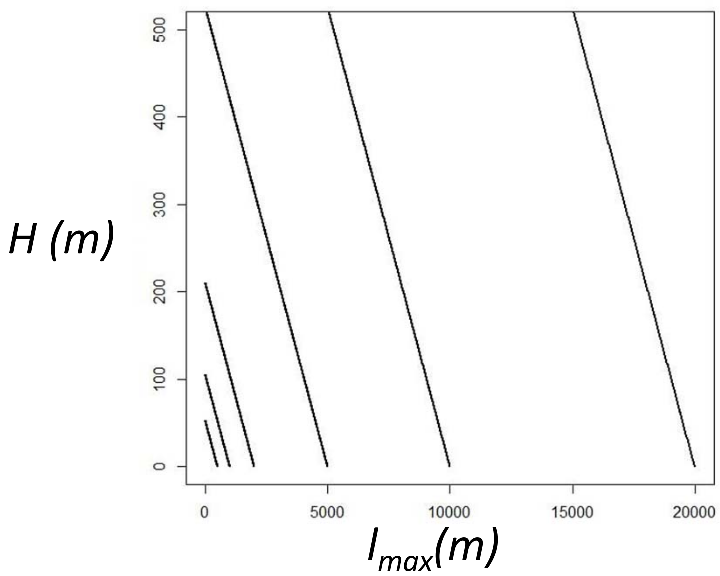

Axisymmetric box model

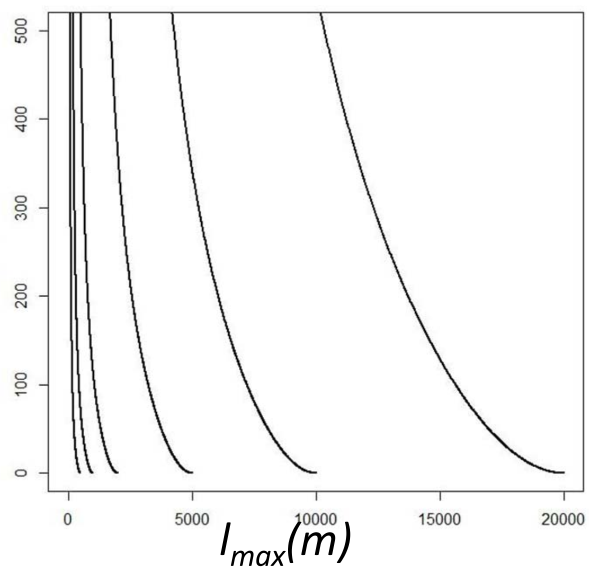

Preliminary probability maps by using the three simplified models

All three maps refer to the **mean probability** values of PDC invasion.

Vents are assumed to open just inland and inside the caldera.

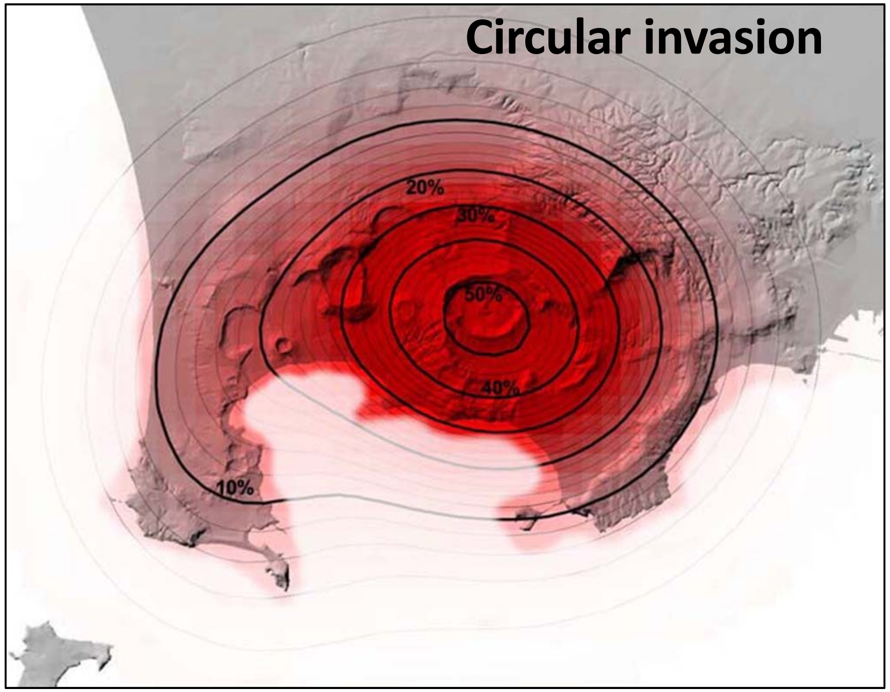

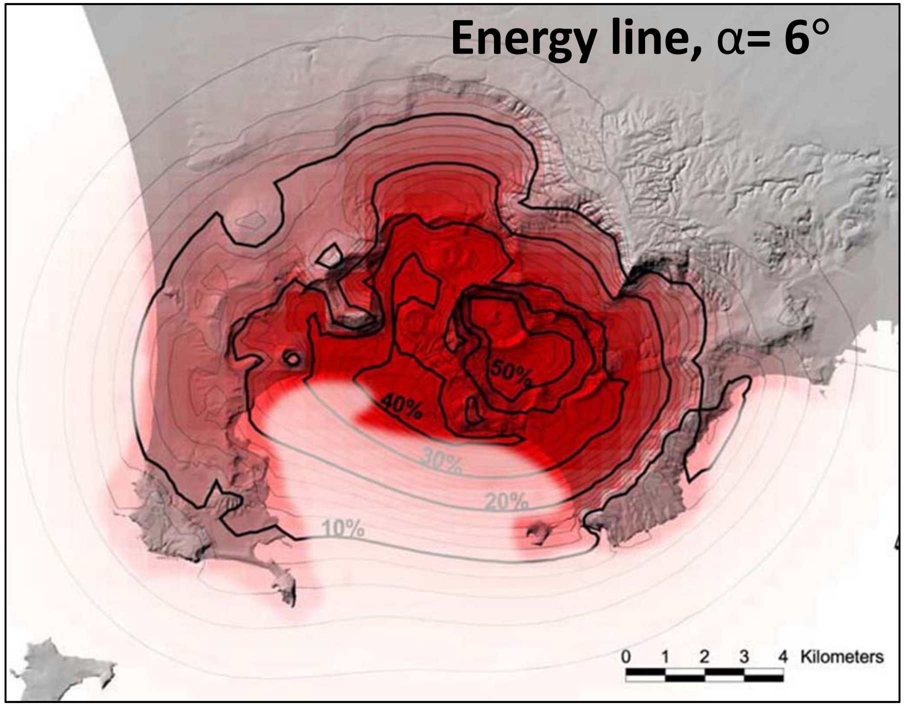

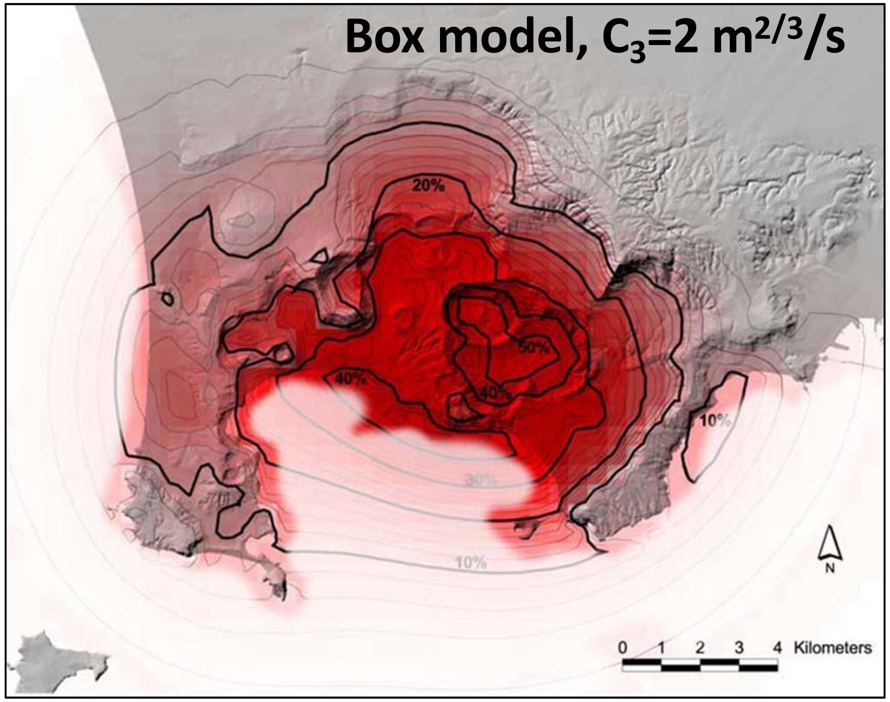

Probability maps by considering the uncertainty on vent locations

The maps represent the **mean and the 5 and 95%ile** considering the **uncertainty on the** probability map of **vent opening.**

The maps were obtained by using the calibrated **box model with C_3 = 2 $m^{2/3}/s$.**

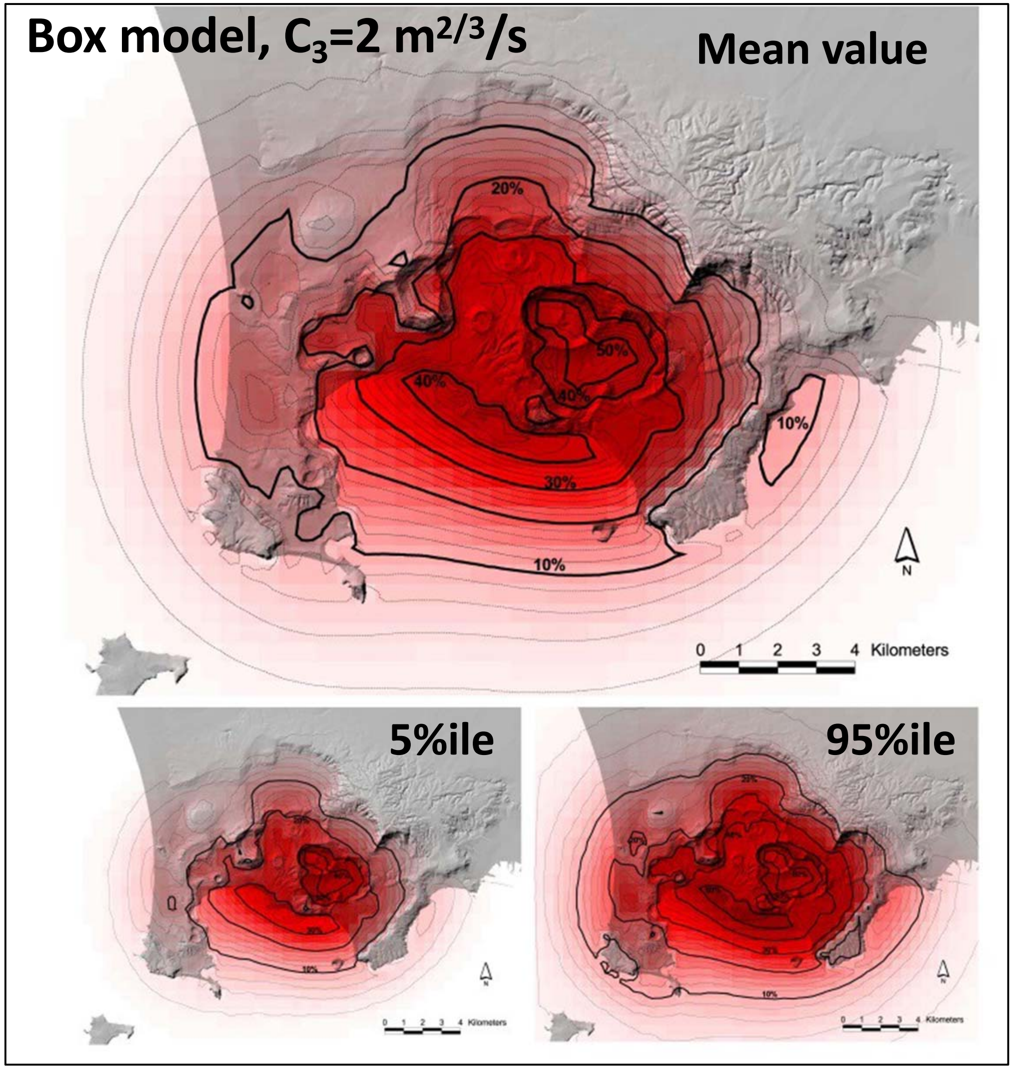

Concluding remarks

- The preliminary hazard maps explicitely consider the **two main unknowns** of the system, i.e. the **vent location** and the **eruption scale**.
- A preliminary **probabilistic map of vent opening**, able to incorporate the associated **uncertainty**, was produced by assigning relative weights to different geological features by using **expert judgement**.
- All the hazard maps produced appear to **capture the first-order features** of the probability of invasion. Main differences are shown along the **caldera rims** where the topographic effect is captured by the **energy line and the calibrated box model**.
- The uncertainty on the probability of **vent location** appears to have a **large effect** on the invasion map.
- Further progress appears to be linked to the use of PDC models able to describe the **3D features of the caldera** and to a better **quantification of the uncertainty sources**.

Acknowlegments

•**Project Speed** “Scenari di pericolosità e danno per i vulcani della Campania”, Dipartimento della Protezione Civile (Italy) and Regione Campania, 2007-2010.

•**Project SAFER** “Services and applications for emergency responses”, European Union, 2010-2012.

•**Project DPC-V1** “Valutazione della pericolosità vulcanica in termini probabilistici”, Dipartimento della Protezione Civile (Italy), 2012-2013.